Physics Letters B 840 (2023) 137837

Contents lists available at ScienceDirect

Physics Letters B

journal homepage: www.elsevier.com/locate/physletb

The triplet Dirac seesaw in the view of the recent CDF-II W mass anomaly

Oleg Popov [a,b], Rahul Srivastava [c,*]

[a] Department of Biology, Shenzhen MSU-BIT University, 1, International University Park Road, Shenzhen 518172, China
[b] Department of Physics, Korea Advanced Institute of Science and Technology, 291 Daehak-ro, Yuseong-gu, Daejeon 34141, Republic of Korea
[c] Department of Physics, Indian Institute of Science Education and Research - Bhopal Bhopal Bypass Road, Bhauri, Bhopal, India

ARTICLE INFO

Article history:
Received 19 April 2022
Received in revised form 1 February 2023
Accepted 7 March 2023
Available online 14 March 2023
Editor: A. Ringwald

ABSTRACT

In the present letter, a Dirac neutrino mass model is presented in the view of the new result on W boson mass of $m_W^{CDF-II} = 80.4335 \pm 0.0094$ GeV, recently reported by the CDF-II experimental collaboration. The newly measured value of the W mass anomaly shows a 7-σ deviation from that predicted by the standard model. The model explains the CDF-II W boson mass anomaly by extending the standard model with hypercharge zero vector-like fermion triplet. Symmetry is amended with a global $U(1)_{B-L}$ which is broken with an hypercharge zero electroweak triplet. It is demonstrated that the model can successfully explain CDF-II result, Dirac neutrino mass origin, while satisfying standard model precision constraints and collider constraints with scalar and fermion triplet masses in the ranger 1.4 TeV−5.2 TeV and 100 TeV -10^{13} GeV, respectively.

1. Introduction

Standard Model (SM) of particle physics has been a highly successful theory with its predictions tested in many different experiments over several decades. The discovery of 125 GeV "SM Higgs like" scalar particle at Large Hadron Collider (LHC) [1,2] seems to complete the SM. However, there is a general expectation that SM cannot be the final theory of nature. One of the main experimental motivation for Beyond Standard Model (BSM) physics comes from the discovery of neutrino oscillations [3]. For neutrinos to oscillate from one flavour to another, neutrinos should have small but tiny masses. Since in SM neutrinos are massless, new physics is necessarily needed to generate small non-zero neutrino masses which can explain neutrino oscillations. In addition, the new result from Collider Detector at Fermilab (CDF) Collaboration taken at Tevatron particle accelerator also indicate that the W boson mass is 7-σ away from the SM predicted value [4] again implying the presence of new physics [5–47]. In this work we aim to provide a coherent new physics description which can simultaneously explains the CDF W-boson anomaly via physics related to neutrino mass generation.

Coming back to possible new physics required to explain CDF anomaly along with generating neutrino mass, one should ask the question about nature of neutrinos i.e. whether they are Dirac or Majorana particles. Experimentally both possibilities are still open as experiments such as neutrinoless double beta decay experiments have not yet seen any signature for Majorana neutrinos [48]. Theoretically, in past most of the research in neutrino physics was focused on Majorana neutrinos [49–58], however in recent times mass models for Dirac neutrinos have garnered quite a bit of attention [59–74]. In this work we will look at the possibility of Dirac neutrino mass models which can also explain the CDF anomaly.

Before moving on to explain the mass models of neutrino physics one should also consider what kind of neutrino mass models can potentially explain the CDF anomaly. Since, the anomaly implies that the W boson mass is larger than the SM prediction.[1] This anomalous

* Corresponding author.
E-mail addresses: opopo001@ucr.edu (O. Popov), rahul@iiserb.ac.in (R. Srivastava).

[1] The numerical SM prediction for W-boson mass is obtained using the experimental values of the precision observable and the SM relationship between them and the W-boson.

https://doi.org/10.1016/j.physletb.2023.137837

behaviour can only be explained by some new physics effecting the W boson mass at tree or loop level. Given the fact that the anomaly is in W boson mass, one can immediately draw some conclusions on the type of new physics required to explain the anomaly. The new physics should be such that it selectively changes the W boson mass but should have minimal or no correction to Z boson mass as neither CDF nor any other experiment has seen any anomaly in Z boson mass. This fact implies that purely neutral particles such as heavy right handed neutrinos will play little to no role in explaining the anomaly, thus restricting the type of neutrino mass models, as we discuss in next section.

The paper is organized as follows: In Section 2 we discuss the different Dirac mass models using the effective operator approach. We identify the Dirac triplet seesaw as the most promising simple candidate. In Section 3 we provide details of the triplet seesaw model and work out the mass spectrum of the particles in the model. In Section 3.1 we show the parameter space of the model which leads to correct neutrino masses consistent with the various neutrino experiments. In Section 3.2 we work out the corrections to the gauge boson masses in our model. In Section 4 we present our results taking into account all the constraints on our model. Finally, we conclude in Section 5.

2. Dirac neutrino mass models

The nature of neutrinos i.e. whether they are Majorana or Dirac particles is still an open question in neutrino physics. The oscillation experiments are insensitive to the Dirac/Majorana nature of neutrinos while the experiments sensitive to neutrino nature such as neutrinoless double beta decay experiments have not seen any signals so far [48]. Traditionally, neutrinos were assumed to be Majorana particles and many different mass mechanisms for them were developed. However, recently the Dirac neutrino mass models have received considerable attention with several novel Dirac neutrino mass mechanism have been developed. Furthermore, several operator based analysis for Dirac neutrino mass models have also been considered in recent past [64,66–69]. To have a successful mass mechanism for Dirac neutrinos several key conditions need to be satisfied:

- If neutrinos are Dirac then right handed neutrinos $\bar{\nu}$ need to be added to SM particle content[2]
- An unbroken symmetry S under which neutrinos transform non-trivially, is needed to ensure that neutrino remain Dirac particles to all quantum loops.
- Tree level coupling between right and left handed neutrinos needs to be forbidden.

Assuming these conditions one can write down the effective operator which will generate the Dirac neutrino masses. The lowest dimensional operator invariant under SM $SU(3)_C \otimes SU(2)_L \otimes U(1)_Y$ gauge symmetries and the S symmetry is given by

$$\frac{\kappa_{ij}}{\Lambda} L_i X_1 X_2 \bar{\nu}_j \tag{1}$$

where κ_{ij} are the dimensionless coupling constants and Λ is the cutoff scale. Also, L_i; $i = 1, 2, 3$ are the SM lepton doublets, $\bar{\nu}_j$; $j = 1, \cdots N$ are the SM gauge singlet right handed neutrinos and X_1, X_2 are VEV carrying scalars whose SM charges should be such that (1) remains invariant under the SM gauge group. There is no constraints on the maximum number of right handed neutrinos, however the neutrino oscillation data implies that at least two neutrinos should be massive, which in turn means that there should be at least two right handed neutrinos. Furthermore, either L or $\bar{\nu}$ or both should be charged under the unbroken symmetry S such that Majorana mass terms to all loops are forbidden. To ensure that S remains unbroken, neither of the two scalars should carry any non-trivial charges under the S symmetry. Finally, either the S symmetry itself or some other mechanism should ensure that the direct coupling between L and $\bar{\nu}$ through SM Higgs doublet H is forbidden.

If one chooses one of the scalars, let's say X_1 in (1), to be the Higgs doublet H i.e. $X_1 \equiv H$, then the $SU(2)_L$ gauge invariance immediately fixes the other scalar X_2 to be either singlet or triplet under the $SU(2)_L$ symmetry. The hypercharge of the scalar X_2 can also be immediately fixed to be $Y = 0$ by the demand that the operator in (1) remains invariant under the $U(1)_Y$ gauge symmetry. Needless to say that none of the scalars X_1, X_2 should carry any non-trivial charge under the $SU(3)_C$ colour symmetry. With the above conditions the two possible dim-5 operators are

$$\begin{aligned} &\frac{\kappa_{ij}}{\Lambda} L_i H \sigma \bar{\nu}_j \\ &\frac{\kappa_{ij}}{\Lambda} L_i H \Delta \bar{\nu}_j \end{aligned} \tag{2}$$

where σ is the $SU(2)_L$ singlet scalar while Δ transforms as a triplet under the $SU(2)_L$ symmetry. The possible Ultra Violet (UV) completions of these operators have been discussed in [64,66,67].

Before going any further with the details of the possible UV completions, let's first discuss the nature and possible examples of the S symmetry which is required to ensure Diracness of the neutrinos. There are many options for the S symmetry which can be a simple abelian discreet symmetry [59–62] or can be a non-abelian discreet symmetry [63], even modular symmetry [74]. Continuous symmetries also can be employed [71]. The simplest option for S seems to be to use the unbroken subgroups of the Lepton number $U(1)_L$ symmetry [59–61,68,70,75]. In this paper we will take this route.

Since, the Lepton number $U(1)_L$ symmetry is anomalous with SM particle content, it is better to consider a linear combination of it with the Baryon number $U(1)_B$ symmetry. The resulting $U(1)_{B-L}$ symmetry can be made anomaly free by addition of three right handed neutrinos. There are two possible solutions namely

[2] We follow the notation where all fermions are left handed. Hence, instead of calling the right handed neutrinos ν_R we define its charge conjugate which will be a left handed field.

Table 1
Model field content and their charges under symmetries of our model. For brevity we have suppressed the flavour indices, see text for details.

	$SU(3)_C$	$SU(2)_L$	$U(1)_Y$	$U(1)_{B-L}$
Q	**3**	**2**	$\frac{1}{6}$	$\frac{1}{3}$
$\overline{u}$	$\overline{\mathbf{3}}$	**1**	$-\frac{2}{3}$	$-\frac{1}{3}$
$\overline{d}$	**3**	**1**	$\frac{1}{3}$	$-\frac{1}{3}$
L	**1**	**2**	$-\frac{1}{2}$	-1
$\overline{e}$	**1**	**1**	1	1
$\overline{\nu}$	**1**	**1**	0	$4, 4, -5$
$\Sigma, \overline{\Sigma}^{\dagger}$	**1**	**3**	0	1
H	**1**	**2**	$\frac{1}{2}$	0
Δ	**1**	**3**	0	-3

- **Vector Solution:** The three right handed neutrinos carry charges $\bar{\nu}_i \sim (-1, -1, -1)$; $i = 1, 2, 3$ under $B - L$ symmetry.
- **Chiral Solution:** The three right handed neutrinos carry charges $\bar{\nu}_i \sim (-4, -4, +5)$; $i = 1, 2, 3$ under $B - L$ symmetry.

In past the vector solution was often used to generate Majorana neutrino masses through the explicit or spontaneous (through a scalar carrying two units of $B - L$ charge) breaking $U(1)_{B-L} \to \mathbb{Z}_2$. However, the chiral solution naturally leads to Dirac neutrino mass models [59–61] with $U(1)_{B-L} \to \mathbb{Z}_3$ explicit or spontaneous breaking. The resulting unbroken $\mathbb{Z}_3$ symmetry can then play the role of the S symmetry and can ensure Dirac nature of neutrinos to all loop orders. Further advantage of using the chiral solution is that the tree level direct coupling between L and $\bar{\nu}$ is automatically forbidden. Finally, being a anomaly free symmetry, $U(1)_{B-L}$ can be trivially gauged leading to a richer phenomenology. There are many possible UV completions of the operators in (2) both at tree and loop level. In this work, keeping CDF anomaly in mind, we will concentrate on a particular solution, namely the Dirac Triplet seesaw model, which we now discuss in details in next section.

3. The Dirac triplet seesaw model

We now focus on a particular seesaw completion of the operator $\frac{\kappa_{ij}}{\Lambda} L_i H \Delta \bar{\nu}_j$ which we call the Dirac triplet seesaw model. The particle content and their charges under $SU(3)_C \otimes SU(2)_L \otimes U(1)_Y$ gauge charges as well as their charges under the global $U(1)_{B-L}$ symmetry are given in Table 1.

As can be seen from Table 1, apart from SM particles we have added three right handed neutrinos which are singlet under SM gauge group but carry $(-4, -4, +5)$ charges under the global $U(1)_{B-L}$ symmetry. In addition we have added two pair of fermions $\Sigma, \bar{\Sigma}$ and a new scalar Δ. Both Σ and Δ carry no colour charge, transform as triplets under $SU(2)_L$ and have zero charge under $U(1)_Y$ symmetry. Furthermore, their $U(1)_{B-L}$ charges are uniquely fixed by the Dirac seesaw mechanism as we discuss in section 3.1.

With the particle content in Table 1 the new Yukawas and total scalar potential Lagrangian are given by

$$\mathcal{L} = -Y_L L \Sigma H - Y_R \overline{\nu} Tr\left[\overline{\Sigma}\Delta\right] - M_\Sigma \Sigma\overline{\Sigma} - V + \text{h.c.}, \tag{3}$$

$$V = m_h^2 H^\dagger H + \frac{\lambda_h}{2}\left(H^\dagger H\right)^2 + \lambda_{h\Delta}\left(H^\dagger H\right) Tr\left(\Delta^\dagger \Delta\right) + \lambda'_{h\Delta}\left(H^\dagger \Delta\Delta^\dagger H\right) \tag{4}$$
$$+ m_\Delta^2 Tr\left(\Delta^\dagger\Delta\right) + \frac{\lambda_\Delta}{2} Tr\left(\Delta^\dagger\Delta\right)^2 + \lambda'_\Delta Tr\left(\Delta^\dagger\Delta\Delta^\dagger\Delta\right) + \mu_H H^\dagger \Delta H.$$

The tree level perturbativity constraints imply that all Yukawas and quartic couplings in (3) and (4) should be less then $\sqrt{4\pi}$. In addition the tree level vacuum stability implies that the matrix of quartic couplings should be co-positive [76]. This implies that the quartic couplings in (4) have to satisfy [77–79]:

$$\lambda_\phi > 0, \qquad \lambda_\Delta + \lambda'_\Delta > 0, \qquad \lambda_\Delta + \frac{\lambda'_\Delta}{3} > 0$$
$$\lambda_{h\Delta} + \sqrt{\lambda_\phi(\lambda_\Delta + \lambda'_\Delta)} > 0, \qquad \lambda_{h\Delta} + \sqrt{\lambda_\phi(\lambda_\Delta + \frac{\lambda'_\Delta}{3})} > 0$$
$$\lambda_{h\Delta} + \lambda'_{h\Delta} + \sqrt{\lambda_\phi(\lambda_\Delta + \lambda'_\Delta)} > 0, \qquad \lambda_{h\Delta} + \lambda'_{h\Delta} + \sqrt{\lambda_\phi(\lambda_\Delta + \frac{\lambda'_\Delta}{3})} > 0. \tag{5}$$

In rest of our analysis we have always maintained both these constraints.

As can be seen from (3) the $SU(2)_L$ triplet fermions couple with both L and $\bar{\nu}$ through Yukawa couplings involving the doublet scalar H and the triplet scalar Δ, respectively. In addition to the Yukawa couplings, the $\Sigma, \bar{\Sigma}$ also have an invariant mass term M_Σ which being independent of the electroweak scale, can be much larger than the vacuum expectation value (VEV) of the scalars i.e. $M_\Sigma \gg v_h, v_\Delta$. Furthermore, the presence of the cubic term $\mu_H H^\dagger \Delta H$ in (4) implies that the global $U(1)_{B-L}$ symmetry is explicitly broken and the Nambu-Goldstone boson gets a mass proportions to μ_H parameter. Additionally, the mass splitting of the neutral and charged components of the triplet scalar is also proportional to $v_\Delta \mu_H$. This leads to strong constraints on scalar masses as discuss in sec. 4.4.

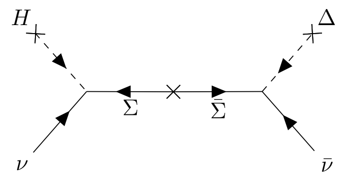

Fig. 1. Tree level Dirac seesaw neutrino mass Feynman diagram. The charge of Δ under $U(1)_{B-L}$ is -3.

3.1. Neutrino masses

The Feynman diagram for the seesaw mass for the neutrinos is given in Fig. 1

Since, the $SU(2)_L$ triplet scalar Δ transform as -3 under the $U(1)_{B-L}$ symmetry, its VEV spontaneously breaks $U(1)_{B-L} \to \mathbb{Z}_3$ residual subgroup. This $\mathbb{Z}_3$ remains unbroken forbidding the Majorana mass terms for neutrinos ensuring the Dirac nature of neutrinos.

The Dirac mass matrix for the neutral fermions is given by

$$M_{\nu\Sigma} = \begin{pmatrix} \nu & \overline{\Sigma} \end{pmatrix} \begin{pmatrix} 0 & Y_L \frac{v_h}{\sqrt{2}} \\ Y_R \frac{v_\Delta}{\sqrt{2}} & M_\Sigma \end{pmatrix} \begin{pmatrix} \overline{\nu} \\ \Sigma \end{pmatrix}, \tag{6}$$

in the $(\nu, \overline{\Sigma})$ (from left) and $(\overline{\nu}, \Sigma)$ (from right) basis, while all Majorana mass terms are forbidden by the residual $\mathbb{Z}_3$ discrete symmetry [64]. Neutrino and the heavy Dirac masses are given by the Dirac seesaw mechanism

$$m_\nu \simeq -Y_L Y_R \frac{v_h v_\Delta}{M_\Sigma}, \tag{7a}$$

$$m_\Sigma \simeq M_\Sigma + Y_L Y_R \frac{v_h v_\Delta}{M_\Sigma}, \tag{7b}$$

where the left and right mixing angles are given by

$$\tan(2\theta_L) = \frac{2\sqrt{2} Y_L v_h M_\Sigma}{Y_L^2 v_h^2 - Y_R^2 v_\Delta^2 - 2M_\Sigma^2}, \tag{8a}$$

$$\tan(2\theta_R) = \frac{2\sqrt{2} Y_R v_\Delta M_\Sigma}{Y_R^2 v_\Delta^2 - Y_L^2 v_h^2 - 2M_\Sigma^2}. \tag{8b}$$

Before ending let us note an interesting feature of our model. As we will discuss shortly, various constraints imply that the VEV of the triplet scalar v_Δ should be far smaller than the VEV of doublet scalar v_h i.e. $v_\Delta << v_h$. This means that the seesaw mass of light neutrinos in (7a) is actually doubly suppressed both by smallness of v_Δ as well as heaviness of M_Σ. This is actually the inverse seesaw limit, an interesting feature of a wide variety of Dirac seesaw models as discussed in [80].

3.2. Gauge boson masses

The addition of the scalar triplet Δ has immediate consequences for the mass of the gauge bosons. The covariant derivative Lagrangian for scalars is given by

$$\mathcal{L} = \left(D_\mu H\right)^\dagger \left(D^\mu H\right) + Tr\left[\left(D_\mu \Delta_{2\times 2}\right)^\dagger \left(D^\mu \Delta_{2\times 2}\right)\right], \tag{9}$$

where

$$D^\mu = \partial^\mu + \imath g W_a^\mu \frac{\sigma^a}{2} + \imath g' \frac{Y}{2} B^\mu, \tag{10}$$

and

$$H = \frac{1}{\sqrt{2}} \begin{pmatrix} H^\pm \\ H^0 \end{pmatrix}, \qquad \langle H \rangle = \frac{1}{\sqrt{2}} \begin{pmatrix} 0 \\ v_h \end{pmatrix}, \tag{11a}$$

$$\Delta = \frac{1}{\sqrt{2}} \begin{pmatrix} \Delta^+ \\ \Delta^0 \\ \Delta^- \end{pmatrix}, \qquad \langle \Delta \rangle = \frac{1}{\sqrt{2}} \begin{pmatrix} 0 \\ v_\Delta \\ 0 \end{pmatrix}, \tag{11b}$$

$$\Delta_{2\times 2} = \begin{pmatrix} \Delta^0/\sqrt{2} & \Delta^+ \\ \Delta^- & -\Delta^0/\sqrt{2} \end{pmatrix}, \qquad \langle \Delta_{2\times 2} \rangle = \langle \Delta_a \rangle \left(\sigma^a\right)_{ij} = \frac{1}{\sqrt{2}} \begin{pmatrix} v_\Delta & 0 \\ 0 & -v_\Delta \end{pmatrix}. \tag{11c}$$

We take the EW doublet VEV, v_h to be the SM VEV v_{SM} ($\equiv 246.221$ GeV), and new the scalar triplet VEV, v_Δ, as the BSM contribution, the sum is $v^2 = v_h^2 + 8v_\Delta^2$. In this case, the SM gauge boson masses and Weinberg angle are given by

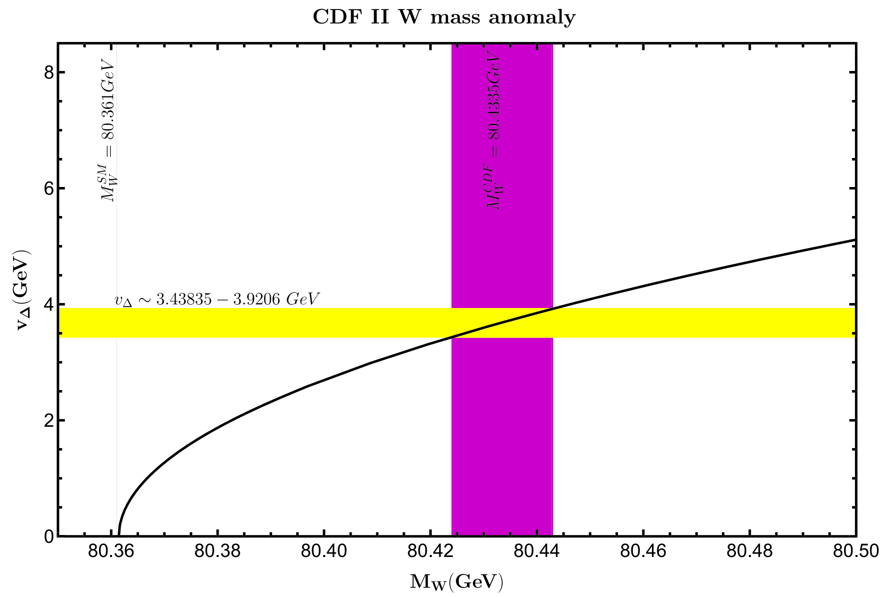

Fig. 2. EW triplet VEV constraints due to recently reported CDF II W mass anomaly [4].

$$M_\gamma = 0, \tag{12a}$$

$$M_Z^2 = \left(g^2 + g'^2\right)\frac{v_h^2}{4}, \tag{12b}$$

$$M_{W^\pm}^2 = \frac{g^2}{4}\left(v_h^2 + 8v_\Delta^2\right), \tag{12c}$$

$$\cos(\theta_W) = \frac{g}{\sqrt{g^2 + g'^2}}, \tag{12d}$$

$$\sin(\theta_W) = \frac{g'}{\sqrt{g^2 + g'^2}}. \tag{12e}$$

As can be seen from (12) the abelian sector is left unaffected, therefore Weinberg angle and Z boson mass remain as in SM. While the extra triplet contributes to the W mass and effects the ρ parameter as will be shown next.

Custodial symmetry violation due to triplet's VEV is given by

$$\rho \equiv \frac{m_W^2}{m_Z^2 \cos^2(\theta_W)} = 1 + 8\frac{v_\Delta^2}{v_h^2}. \tag{13}$$

The most recent PDG value of $\rho_{exp} = 1.00038 \pm 0.00020$ [81] has to be scaled by a factor of $\left(m_W^{CDF}/m_W^{PDG}\right)^2$ to give updated value of $\rho \simeq 1.00219 \pm 0.00044$ after including the CDF results. Using (13) gives $v_\Delta \simeq 4.06997 \pm 0.26529$ GeV, which in turn is consistent with the triplet VEV of Fig. 2, to be obtained directly from the m_W^{CDF} value fit in Sec. 4.1.

4. Analysis and constraints

Below we discuss the relevant constraints on the model, including neutrino mass, EW precision, and current and future collider constraints.

4.1. CDF II W mass anomaly

Recent reported result by CDF II collaboration differs from SM value by 7-σ. In order to explain this deviation with a scalar triplet model $\langle\Delta\rangle \ll \langle H\rangle$. This fits naturally into the (Dirac) triplet seesaw mechanism. The range of valid EW triplet VEV is between $3.4384\ GeV < \langle\Delta\rangle < 3.9206\ GeV$ and is shown in Fig. 2.

4.2. Neutrino mass constraints

Dirac seesaw neutrino mass is given by (7a). The natural way to satisfy the small neutrino masses is the combination of small scalar triplet VEV and large ($\gg \langle H\rangle$) fermion triplet mass. The correlation between relevant parameters is shown in Fig. 3. As can be seen from the figure for the Yukawas of the order $\mathcal{O}(0.1)$ the fermion triplet must be of the order $\mathcal{O}\left(10^{10-11}\right)$ GeV to satisfy the neutrino mass constraint. On the other hand, if Yukawas are of the order $\mathcal{O}\left(10^{-4}\right)$ then the heavy fermion triplet can be as light as $\mathcal{O}(10-100)$ TeV, which brings it into a detectable range for future hadronic/leptonic colliders (100 TeV collider or FFC).

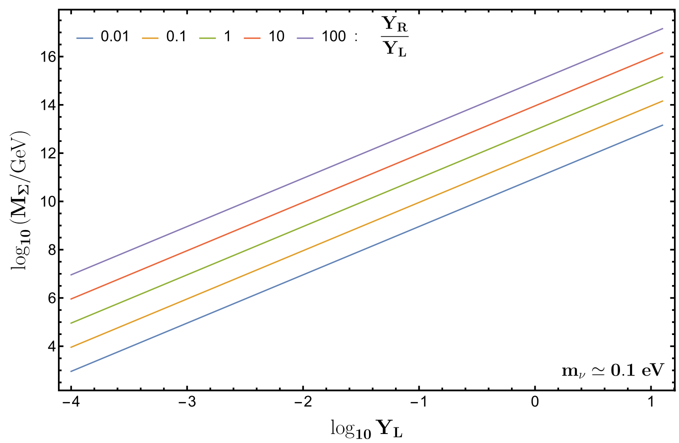

Fig. 3. Correlation between M_Σ and $Y_{L,R}$, for various ratios of Y_L/Y_R, that satisfy the observed neutrino mass.

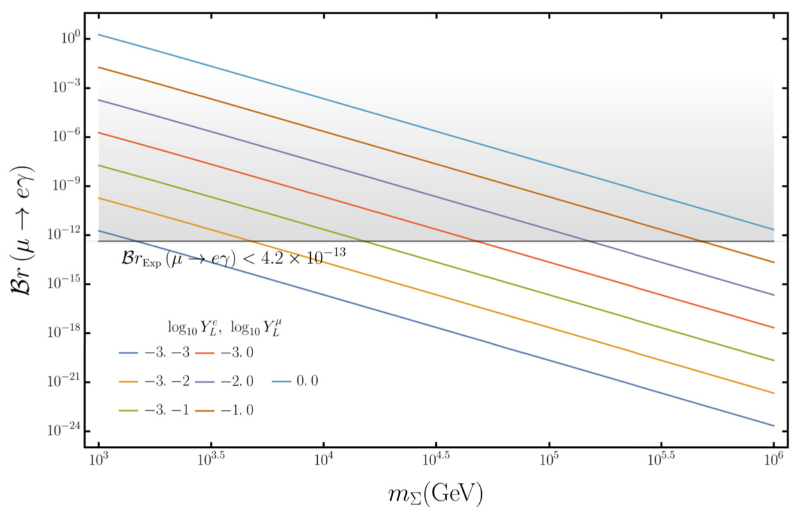

Fig. 4. Plot for m_Σ vs $\mathcal{B}r(\mu \to e\gamma)$ plot for various values of $Y_L^{e,\mu}$ Yukawa couplings. Gray shaded region on the plot indicates the ruled-out region by the experiments.

4.3. Constraints from lepton flavor violation

Most up-to-date experimental limit on $\mu \to e\gamma$ is $\mathcal{B}r(\mu \to e\gamma) < 4.2 \times 10^{-13}$ from MEG Collaboration [82]. In our model main contribution comes from the Yukawa $\bar{L}\Sigma H$ interaction involving the Leptonic doublet (L), the fermionic triplet (Σ) and the Higgs doublet (H). The Branching Ratio ($Br(\mu \to e\gamma)$) as function of the triplet mass (m_Σ) and benchmark values of the Yukawa coupling are shown in Fig. 4. Note that m_Σ in our model is also constrained by the limits coming from neutrino mass, refer to Fig. 3, which implies that for the allowed choices of Yukawa coupling and m_Σ, the $\mu \to e\gamma$ process gives a weak constraint only.

4.4. Bounds from electroweak precision experiments

The most important relevant electroweak precision constraints (EWPC) are the oblique, *aka* Peskin-Takeuchi [83] S, T, U parameters [84–86], which represent the contribution of BSM physics to the SM gauge sector. Since the triplet scalar carries no hypercharge, its contribution to S parameter is absent. On the other hand, the triplet fermion contributes to S, T, U parameters only at the loop order. Furthermore, since the BSM EW triplet fermion is expected to be much heavier than the EW scale, its contribution to S, T, U oblique parameters is expected to be of subleading order. As a result of the above, new physics contribution to S, T, U parameters from scalar triplet with zero hypercharge is given by [87,88]

$$S \simeq 0, \tag{14a}$$

$$\begin{aligned} T &= \frac{1}{8\pi}\frac{1}{\sin^2\theta_W \cos^2\theta_W}\left[\frac{M_{\Delta^0}^2 + M_{\Delta^\pm}^2}{M_Z^2} - \frac{2M_{\Delta^0}^2 M_{\Delta^\pm}^2}{M_Z^2\left(M_{\Delta^0}^2 - M_{\Delta^\pm}^2\right)}\log\left(\frac{M_{\Delta^0}^2}{M_{\Delta^\pm}^2}\right)\right], \\ &\simeq \frac{1}{8\pi}\frac{1}{\sin^2\theta_W \cos^2\theta_W}\frac{(\Delta M)^2}{M_Z^2}, \end{aligned} \tag{14b}$$

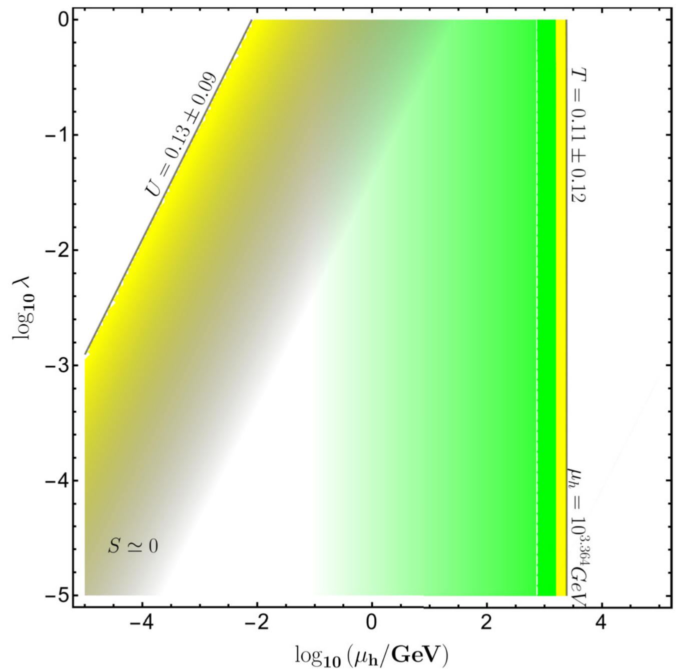

Fig. 5. T and U Peskin-Takeuchi constraints on the model parameters. Green (yellow) shading corresponds to 1(2) standard deviation bounds from updated global SM fits (eq. 15). $S \simeq 0$ since there is no BSM physics contribution to the Z-boson. $\lambda_{H\Delta}, \lambda'_{H\Delta} \ll \lambda_\Delta = \lambda'_\Delta = \lambda$ is taken here.

$$U = -\frac{1}{3\pi}\left(M^4_{\Delta^0}\log\left(\frac{M^2_{\Delta^0}}{M^2_{\Delta^\pm}}\right)\frac{\left(3M^2_{\Delta^\pm}-M^2_{\Delta^0}\right)}{\left(M^2_{\Delta^0}-M^2_{\Delta^\pm}\right)^3}+\frac{5\left(M^4_{\Delta^0}+M^4_{\Delta^\pm}\right)-22M^2_{\Delta^0}M^2_{\Delta^\pm}}{6\left(M^2_{\Delta^0}-M^2_{\Delta^\pm}\right)^2}\right)$$
$$\simeq \frac{\Delta M}{3\pi M_{\Delta^\pm}}, \tag{14c}$$

where $\Delta M = M_{\Delta^\pm} - M_{\Delta^0}$ and $\Delta M \ll M_{\Delta^\pm,\Delta^0}$ in the limit $M_{\Delta^\pm,\Delta^0} \gg M_h$.

The current global fit of electroweak precision data (EWPD) after including the CDF result, gives [6]

$$S = 0.06 \pm 0.10, \tag{15a}$$
$$T = 0.11 \pm 0.12, \tag{15b}$$
$$U = 0.13 \pm 0.09. \tag{15c}$$

The oblique parameter constraints for the present model are shown in Fig. 5. As can be seen from the plot, the most important constraint comes from T parameter and gives an upper limit on $\mu_H \simeq 2.3$ TeV parameter of the scalar potential. Further, the region of very small μ_H (≤ 10 MeV) is excluded for $10^{-3} < \lambda_\Delta = \lambda'_\Delta = \lambda$ in the two sigma range. For the demonstration purposes we took $\lambda_{H\Delta}, \lambda'_{H\Delta} \ll \lambda_\Delta = \lambda'_\Delta = \lambda$ in Fig. 5.

4.5. Collider constraints

We now look at the main constraints coming from collider physics. The first constraint we consider is the constraint coming from $h \to \gamma\gamma$ decay, where the new charged particles present in our model will also contribute. In our model the main contribution to $h \to \gamma\gamma$ comes from the charged components of the scalar triplet Δ and the fermionic triplet Σ running in the loop. Since, the allowed parameter space from other constraints (neutrino mass, Fig. 3, and μ_h, Fig. 7) implies that Δ is much lighter than Σ, the charged scalar component of Δ will give us the dominant contribution to $h \to \gamma\gamma$ as shown in the Fig. 6.

Since the model contains no BSM singlet particle, all new physics is subject to stringent collider constraints from LHC. Furthermore, the proposed future colliders such as FCC and future lepton collider can further probe the EW scalar and fermionic triplets of our model. The most up-to-date limit on the fermion EW triplet comes from the CMS collaboration and is given by $M_\Sigma > 574$ GeV [89]. Whereas, the current LHC limit on the charged component of the scalar EW triplet is given by $m_{\Delta^{\pm,0}} > 1065$ GeV [90]. The proposed FCC can potentially improve the limits on scalar EW triplet upto $m_{\Delta^{\pm,0}} > 1.4$ TeV [86]. The combination of the strongest collider bound and the oblique parameter constraints is shown in Fig. 7. As can be seen from this figure, the only valid parameter window for this model left is given by 177.8 $GeV < \mu_H < 2312$ GeV. Which translates into 1.4 $TeV < m_\Delta < 5.19$ TeV bounds on scalar EW triplet for $\Delta m_\Delta \ll m_{\Delta^\pm} \approx m_{\Delta^0} \approx m_\Delta$ approximation, as can be seen from the Fig. 7.

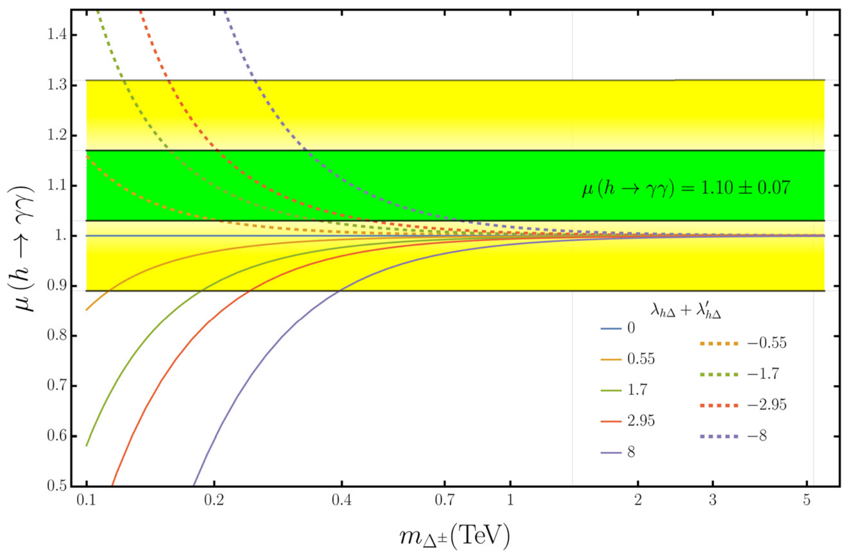

Fig. 6. $m_{\Delta^\pm}$ vs $\mu\,(h \to \gamma\gamma)$ plot for different values of $\lambda_{h\Delta} + \lambda'_{h\Delta}$, higgs quartic coupling constants. Green and yellow shaded regions indicate the 1σ and 3σ deviations from the PDG experimental average, $\mu\,(h \to \gamma\gamma) = 1.10 \pm 0.07$ [81], respectively. The collider constraint on $\Delta^\pm$'s mass for present model is 1.4 TeV $< m_{\Delta^\pm} <$ 5.19 TeV.

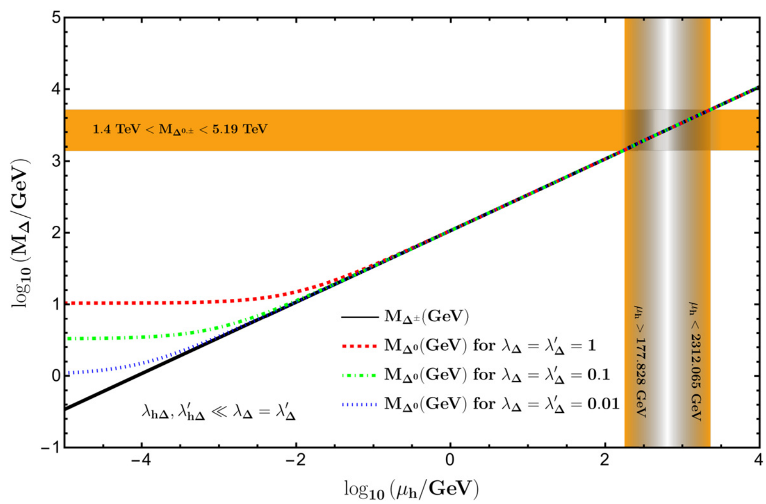

Fig. 7. Mass constraints on the charged and neutral EW scalar triplet components. Upper limit is due to T oblique parameter constraint, while the lower limit is due to LHC and FCC constraints.

Regarding the detectability of the new particles, there are several novel channels for the production and decay modes of the new particles in our model. The list of the leading ones along with the dependence on the couplings and masses of the new particles is given in appendix A. Where more detailed information on the production and decay of the new BSM particles, Δ scalar and Σ fermionic EW triplets, in the current (LHC) and future (FCC) colliders is provided.

Finally, one may wonder if we can relate the W-boson mass anomaly with other anomalies like the muon $g-2$ anomaly [91]. Unfortunately, in our current model, which is a minimal model, all the new particles are quite heavy and hence their effect on μ_{g-2} is be negligible. To explain the muon $g-2$ anomaly one typically needs new particle(s) which are of low mass [92]. However, one can indeed extend our minimal model so that muon $g-2$ anomaly can also be explained. One natural extension will be to have induced VEV for the triplet scalar like done in [67], where new $SU(2)_L$ singlet scalars can be light and can be used to explain the muon $g-2$ anomaly. We plan to study such extensions in future works on the model.

5. Conclusion

In the present letter, a model based on the scalar and fermion EW triplet was presented. The model is shown to successfully generate naturally small Dirac neutrino masses via a Dirac seesaw mechanism with a spontaneous symmetry breaking of the global $U(1)_{B-L}$ symmetry. Furthermore, the model successfully reproduces the 7-σ W mass anomaly recently reported by CDF II collaboration. After applying all relevant constraints, including neutrino mass, W mass anomaly, and electroweak precision constraints, it is shown that the scalar triplet with hypercharge zero should have a mass in the range between 1.4 TeV and 5.19 TeV, whereas the new fermion triplet can have a mass anywhere from 100 TeV and up to 10^{13} GeV.

Declaration of competing interest

The authors declare the following financial interests/personal relationships which may be considered as potential competing interests: Rahul Srivastava reports financial support was provided by Government of India, SERB Startup Grant. Oleg Popov reports financial support was provided by Samsung Science and Technology Foundation.

Data availability

Data will be made available on request.

Acknowledgements

OP was supported by the Samsung Science and Technology Foundation under Grant No. SSTF-BA1602-04 and National Research Foundation of Korea under Grant Number 2018R1A2B6007000. RS is supported by the Government of India, SERB Startup Grant No. SRG/2020/002303. All Feynman diagrams were created using TikZ-Feynman LateX package [93].

Appendix A. Production and decay channels of the new particles

The diagrams contributing to Δ and Σ triplet production are divided into two groups by production type, $q - \bar{q}$ vs gluon gluon fusion, and into two further subgroups based on whether or not they involve mixing between the new particles and their SM counterparts. Some of the leading contributions to the amplitude $\mathcal{A}$ for single production are shown in Figs. 8b, 8c, 9a, 9b, 10b, 11b and 8a, 9e, 10a, 11a for scalar triplet Δ and fermion triplet Σ, respectively. Similarly, double production for scalar triplet Δ and fermion triplet Σ are shown in Figs. 9g and 8d, respectively.

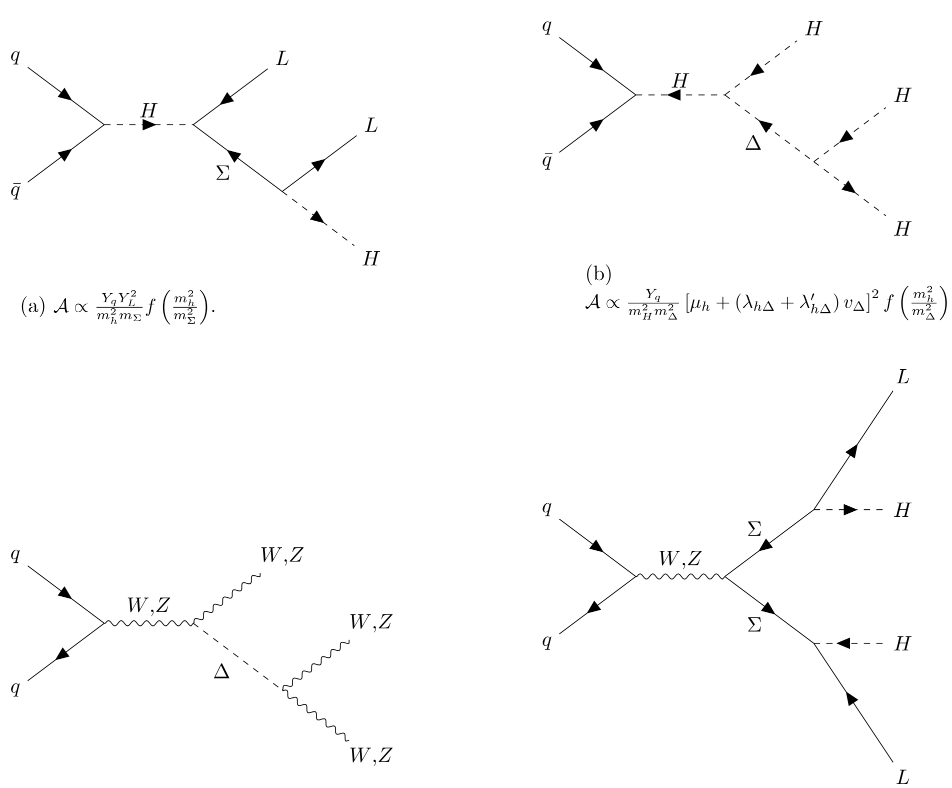

(a) $\mathcal{A} \propto \frac{Y_q Y_L^2}{m_h^2 m_\Sigma} f\left(\frac{m_h^2}{m_\Sigma^2}\right)$.

(b) $\mathcal{A} \propto \frac{Y_q}{m_H^2 m_\Delta^2}\left[\mu_h + (\lambda_{h\Delta} + \lambda'_{h\Delta})\, v_\Delta\right]^2 f\left(\frac{m_h^2}{m_\Delta^2}\right)$.

(c) $\mathcal{A} \propto \frac{g^5 v_\Delta^2}{m_{W,Z}^2 m_\Delta^2} f\left(\frac{m_{W,Z}^2}{m_\Delta^2}\right)$.

(d) $\mathcal{A} \propto \frac{g^2 Y_L^2}{m_{W,Z}^2 m_\Sigma^2} f\left(\frac{m_h^2}{m_\Sigma^2}\right)$.

Fig. 8. Dominant quark anti-quark fusion feynman diagrams contributing to the production of Δ and Σ scalar and fermion EW triplets, respectively, that involve no mixing. The SM particles will proceed with their usual SM decay modes.

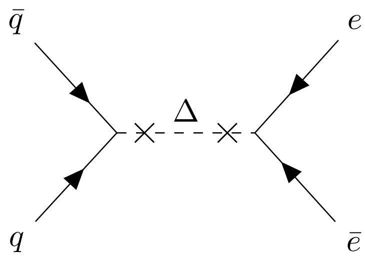

(a) $\mathcal{A} \propto Y_q Y_e \frac{\left[\mu_h v_h + \left(\lambda_{h\Delta}+\lambda'_{h\Delta}\right) v_h v_\Delta\right]^2}{\left(m_\Delta^2 - m_h^2\right)^2 m_\Delta^2}$.

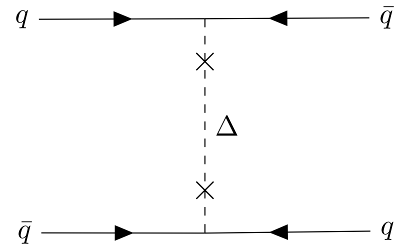

(b) $\mathcal{A} \propto Y_q Y_q \frac{\left[\mu_h v_h + \left(\lambda_{h\Delta}+\lambda'_{h\Delta}\right) v_h v_\Delta\right]^2}{\left(m_\Delta^2 - m_h^2\right)^2 m_\Delta^2}$.

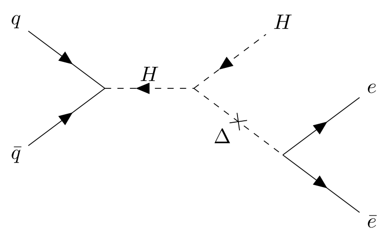

(c)
$\mathcal{A} \propto \frac{Y_q Y_e}{v_h m_h^2 m_\Delta^2} \frac{\left[\mu_h v_h + \left(\lambda_{h\Delta}+\lambda'_{h\Delta}\right) v_h v_\Delta\right]^2}{\left(m_\Delta^2 - m_h^2\right)}$
with $m_\Sigma > m_\Delta$.

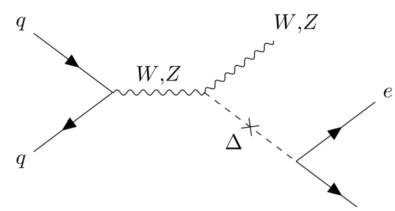

(d)
$\mathcal{A} \propto g^3 Y_e v_\Delta \frac{\left[\mu_h v_h + \left(\lambda_{h\Delta}+\lambda'_{h\Delta}\right) v_h v_\Delta\right]}{m_{W,Z}^2 m_\Delta^2 (m_\Delta^2 - m_h^2)}$.

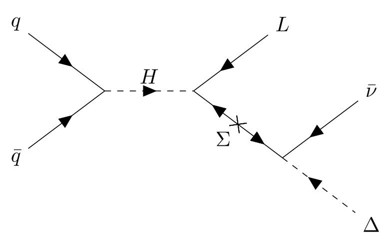

(e) $\mathcal{A} \propto \frac{Y_q Y_l Y_R}{m_h^2 m_\Sigma} f\left(\frac{m_h^2}{m_\Sigma^2}\right)$.

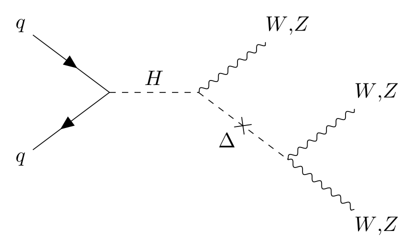

(f)
$\mathcal{A} \propto \frac{g^3 Y_q v_\Delta \left[\mu_h v_h + \left(\lambda_{h\Delta}+\lambda'_{h\Delta}\right) v_h v_\Delta\right]}{m_h^2 m_\Delta^2 \left(m_\Delta^2 - m_h^2\right)} f\left(\frac{m_h^2}{m_\Delta^2}\right)$.

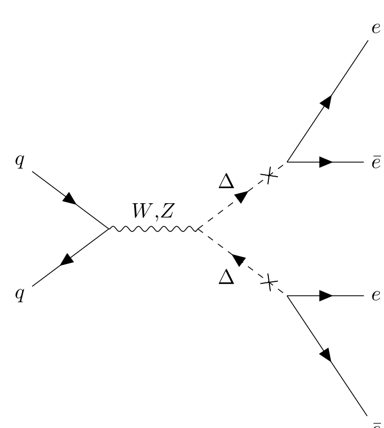

(g)
$\mathcal{A} \propto g^2 Y_e^2 \frac{\left[\mu_h v_h + \left(\lambda_{h\Delta}+\lambda'_{h\Delta}\right) v_h v_\Delta\right]^2}{m_{W,Z}^2 m_\Delta^4} f\left(\frac{m_h^2}{m_\Delta^2}\right)$.

Fig. 9. Dominant quark anti-quark fusion feynman diagrams contributing to the production of Δ and Σ scalar and fermion EW triplets, respectively, that involve mixing. The crosses in the feynman diagrams indicate the mixing between new BSM scalars/fermions with the their SM scalars/leptonic counterparts. The SM particles will proceed with their usual SM decay modes.

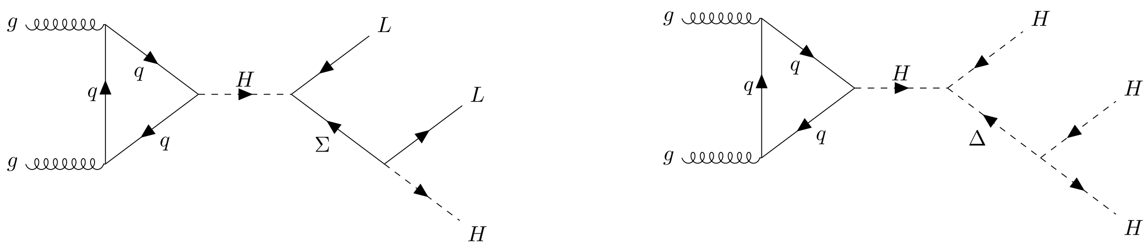

(a) $\mathcal{A} \propto \frac{g_s^2}{16\pi^2}\frac{Y_q Y_L^2}{m_h^2 m_\Sigma} f\left(\frac{m_h^2}{m_\Sigma^2}\right)$.

(b) $\mathcal{A} \propto \frac{g_s^2}{16\pi^2} Y_q \frac{\left[\mu_h+\left(\lambda_{h\Delta}+\lambda'_{h\Delta}\right)v_\Delta\right]^2}{m_H^2 m_\Delta^2} f\left(\frac{m_h^2}{m_\Delta^2}\right)$.

Fig. 10. Dominant gluon gluon fusion feynman diagrams contributing to the production of Δ and Σ scalar and fermion EW triplets, respectively, that involve no mixing. The SM particles will proceed with their usual SM decay modes. Note that there are other feynman diagrams, similar to those given in Fig. 8, which will also contribute to gluon gluon fusion.

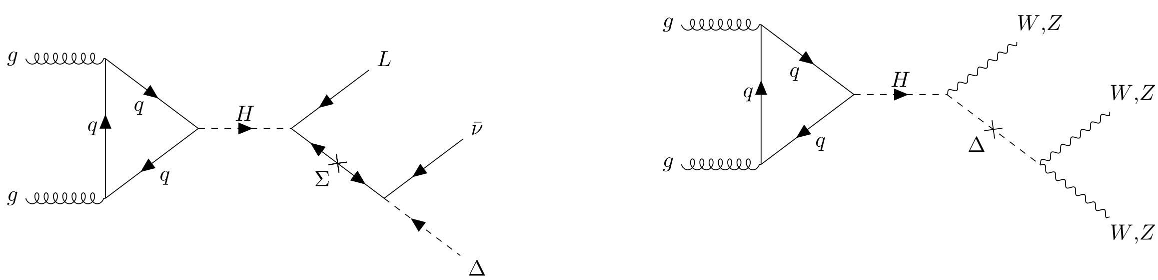

(a) $\mathcal{A} \propto \frac{g_s^2}{16\pi^2}\frac{Y_q Y_l Y_R}{m_h^2 M_\Sigma} f\left(\frac{m_h^2}{m_\Sigma^2}\right)$.

(b) $\mathcal{A} \propto \frac{g_s^2}{16\pi^2}\frac{g^3 Y_q\left[\mu_h v_h+\left(\lambda_{h\Delta}+\lambda'_{h\Delta}\right)v_h v_\Delta\right]v_\Delta}{m_h^2 m_\Delta^2} f\left(\frac{m_h^2}{m_\Delta^2}\right)$.

Fig. 11. Dominant gluon gluon fusion feynman diagrams contributing to the production of Δ and Σ scalar and fermion EW triplets, respectively, that involve mixing. The crosses in the feynman diagrams indicate the mixing between new BSM scalars/fermions with the their SM scalars/leptonic counterparts. The SM particles will proceed with their usual SM decay modes. Note that there are other feynman diagrams, similar to those given in Fig. 9, which will also contribute to gluon gluon fusion.

References

[1] G. Aad, et al., ATLAS, Phys. Lett. B 716 (2012) 1, arXiv:1207.7214 [hep-ex].
[2] S. Chatrchyan, et al., CMS, Phys. Lett. B 716 (2012) 30, arXiv:1207.7235 [hep-ex].
[3] Y. Fukuda, et al., Super-Kamiokande, Phys. Rev. Lett. 81 (1998) 1562, arXiv:hep-ex/9807003.
[4] T. Aaltonen, et al., CDF, Science 376 (2022) 170.
[5] Y.-Z. Fan, T.-P. Tang, Y.-L.S. Tsai, L. Wu, arXiv:2204.03693 [hep-ph], 2022.
[6] C.-T. Lu, L. Wu, Y. Wu, B. Zhu, arXiv:2204.03796 [hep-ph], 2022.
[7] P. Athron, A. Fowlie, C.-T. Lu, L. Wu, Y. Wu, B. Zhu, arXiv:2204.03996 [hep-ph], 2022.
[8] G.-W. Yuan, L. Zu, L. Feng, Y.-F. Cai, arXiv:2204.04183 [hep-ph], 2022.
[9] A. Strumia, arXiv:2204.04191 [hep-ph], 2022.
[10] J.M. Yang, Y. Zhang, arXiv:2204.04202 [hep-ph], 2022.
[11] J. de Blas, M. Pierini, L. Reina, L. Silvestrini, arXiv:2204.04204 [hep-ph], 2022.
[12] C.-R. Zhu, M.-Y. Cui, Z.-Q. Xia, Z.-H. Yu, X. Huang, Q. Yuan, Y.Z. Fan, arXiv:2204.03767 [astro-ph.HE], 2022.
[13] X.K. Du, Z. Li, F. Wang, Y.K. Zhang, arXiv:2204.04286 [hep-ph], 2022.
[14] T.-P. Tang, M. Abdughani, L. Feng, Y.-L.S. Tsai, Y.-Z. Fan, arXiv:2204.04356 [hep-ph], 2022.
[15] G. Cacciapaglia, F. Sannino, arXiv:2204.04514 [hep-ph], 2022.
[16] M. Blennow, P. Coloma, E. Fernández-Martínez, M. González-López, arXiv:2204.04559 [hep-ph], 2022.
[17] K. Sakurai, F. Takahashi, W. Yin, arXiv:2204.04770 [hep-ph], 2022.
[18] J. Fan, L. Li, T. Liu, K.-F. Lyu, arXiv:2204.04805 [hep-ph], 2022.
[19] X. Liu, S.-Y. Guo, B. Zhu, Y. Li, arXiv:2204.04834 [hep-ph], 2022.
[20] H.M. Lee, K. Yamashita, arXiv:2204.05024 [hep-ph], 2022.
[21] Y. Cheng, X.-G. He, Z.-L. Huang, M.-W. Li, arXiv:2204.05031 [hep-ph], 2022.
[22] E. Bagnaschi, J. Ellis, M. Madigan, K. Mimasu, V. Sanz, T. You, arXiv:2204.05260 [hep-ph], 2022.
[23] A. Paul, M. Valli, arXiv:2204.05267 [hep-ph], 2022.
[24] H. Bahl, J. Braathen, G. Weiglein, arXiv:2204.05269 [hep-ph], 2022.
[25] P. Asadi, C. Cesarotti, K. Fraser, S. Homiller, A. Parikh, arXiv:2204.05283 [hep-ph], 2022.
[26] L. Di Luzio, R. Gröber, P. Paradisi, arXiv:2204.05284 [hep-ph], 2022.
[27] P. Athron, M. Bach, D.H.J. Jacob, W. Kotlarski, D. Stöckinger, A. Voigt, arXiv:2204.05285 [hep-ph], 2022.
[28] J. Gu, Z. Liu, T. Ma, J. Shu, arXiv:2204.05296 [hep-ph], 2022.
[29] J.J. Heckman, arXiv:2204.05302 [hep-ph], 2022.
[30] K.S. Babu, S. Jana, Vishu P.K., arXiv:2204.05303 [hep-ph], 2022.
[31] B.-Y. Zhu, S. Li, J.-G. Cheng, R.-L. Li, Y.-F. Liang, arXiv:2204.04688 [astro-ph.HE], 2022.
[32] R. Balkin, E. Madge, T. Menzo, G. Perez, Y. Soreq, J. Zupan, arXiv:2204.05992 [hep-ph], 2022.
[33] T. Biekötter, S. Heinemeyer, G. Weiglein, arXiv:2204.05975 [hep-ph], 2022.
[34] M. Endo, S. Mishima, arXiv:2204.05965 [hep-ph], 2022.
[35] A. Crivellin, M. Kirk, T. Kitahara, F. Mescia, arXiv:2204.05962 [hep-ph], 2022.

[36] K. Cheung, W.-Y. Keung, P.-Y. Tseng, arXiv:2204.05942 [hep-ph], 2022.
[37] X.K. Du, Z. Li, F. Wang, Y.K. Zhang, arXiv:2204.05760 [hep-ph], 2022.
[38] Y. Heo, D.-W. Jung, J.S. Lee, arXiv:2204.05728 [hep-ph], 2022.
[39] N.V. Krasnikov, arXiv:2204.06327 [hep-ph], 2022.
[40] Y.H. Ahn, S.K. Kang, R. Ramos, arXiv:2204.06485 [hep-ph], 2022.
[41] X.-F. Han, F. Wang, L. Wang, J.M. Yang, Y. Zhang, arXiv:2204.06505 [hep-ph], 2022.
[42] M.-D. Zheng, F.-Z. Chen, H.-H. Zhang, arXiv:2204.06541 [hep-ph], 2022.
[43] P.F. Perez, H.H. Patel, A.D. Plascencia, arXiv:2204.07144 [hep-ph], 2022.
[44] A. Ghoshal, N. Okada, S. Okada, D. Raut, Q. Shafi, A. Thapa, arXiv:2204.07138 [hep-ph], 2022.
[45] J. Kawamura, S. Okawa, Y. Omura, arXiv:2204.07022 [hep-ph], 2022.
[46] K.I. Nagao, T. Nomura, H. Okada, arXiv:2204.07411 [hep-ph], 2022.
[47] S. Kanemura, K. Yagyu, arXiv:2204.07511 [hep-ph], 2022.
[48] S. Abe, et al., KamLAND-Zen, arXiv:2203.02139 [hep-ex], 2022.
[49] P. Minkowski, Phys. Lett. B 67 (1977) 421.
[50] T. Yanagida, in: O. Sawada, A. Sugamoto (Eds.), KEK., Tsukuba, 1979, p. 95.
[51] M. GellMann, P. Ramond, R. Slansky, in: P. van Nieuwenhuizen, D.Z. Freedman (Eds.), Supergravity, North-Holland, Amsterdam, 1979, p. 315.
[52] R.N. Mohapatra, G. Senjanovic, Phys. Rev. Lett. 44 (1980) 912 [231(1979)].
[53] J. Schechter, J.W.F. Valle, Phys. Rev. D 22 (1980) 2227.
[54] R. Foot, H. Lew, X.G. He, G.C. Joshi, Z. Phys. C 44 (1989) 441.
[55] A. Zee, Phys. Lett. B 93 (1980) 389, Phys. Lett. B 95 (1980) 461, Erratum.
[56] K.S. Babu, Phys. Lett. B 203 (1988) 132.
[57] E. Ma, Phys. Rev. D 73 (2006) 077301, arXiv:hep-ph/0601225.
[58] S. Fraser, E. Ma, O. Popov, Phys. Lett. B 737 (2014) 280, arXiv:1408.4785 [hep-ph].
[59] E. Ma, R. Srivastava, Phys. Lett. B 741 (2015) 217, arXiv:1411.5042 [hep-ph].
[60] E. Ma, R. Srivastava, Mod. Phys. Lett. A 30 (2015) 1530020, arXiv:1504.00111 [hep-ph].
[61] E. Ma, N. Pollard, R. Srivastava, M. Zakeri, Phys. Lett. B 750 (2015) 135, arXiv:1507.03943 [hep-ph].
[62] S. Centelles Chuliá, E. Ma, R. Srivastava, J.W.F. Valle, Phys. Lett. B 767 (2017) 209, arXiv:1606.04543 [hep-ph].
[63] S. Centelles Chuliá, R. Srivastava, J.W.F. Valle, Phys. Lett. B 761 (2016) 431, arXiv:1606.06904 [hep-ph].
[64] E. Ma, O. Popov, Phys. Lett. B 764 (2017) 142, arXiv:1609.02538 [hep-ph].
[65] S. Centelles Chuliá, R. Srivastava, J.W.F. Valle, Phys. Lett. B 773 (2017) 26, arXiv:1706.00210 [hep-ph].
[66] S. Centelles Chuliá, R. Srivastava, J.W.F. Valle, Phys. Lett. B 781 (2018) 122, arXiv:1802.05722 [hep-ph].
[67] S. Centelles Chuliá, R. Srivastava, J.W.F. Valle, Phys. Rev. D 98 (2018) 035009, arXiv:1804.03181 [hep-ph].
[68] C. Bonilla, S. Centelles-Chuliá, R. Cepedello, E. Peinado, R. Srivastava, Phys. Rev. D 101 (2020) 033011, arXiv:1812.01599 [hep-ph].
[69] S. Centelles Chuliá, R. Cepedello, E. Peinado, R. Srivastava, J. High Energy Phys. 10 (2019) 093, arXiv:1907.08630 [hep-ph].
[70] R. Srivastava, C. Bonilla, E. Peinado, Lett. High Energy Phys. 2 (2019) 124, arXiv:1903.01477 [hep-ph].
[71] E. Peinado, M. Reig, R. Srivastava, J.W.F. Valle, Mod. Phys. Lett. A 35 (2020) 2050176, arXiv:1910.02961 [hep-ph].
[72] S.K. Kang, O. Popov, Phys. Rev. D 98 (2018) 115025, arXiv:1807.07988 [hep-ph].
[73] A. Dasgupta, S.K. Kang, O. Popov, Phys. Rev. D 100 (2019) 075030, arXiv:1903.12558 [hep-ph].
[74] A. Dasgupta, T. Nomura, H. Okada, O. Popov, M. Tanimoto, arXiv:2111.06898 [hep-ph], 2021.
[75] M. Hirsch, R. Srivastava, J.W.F. Valle, Phys. Lett. B 781 (2018) 302, arXiv:1711.06181 [hep-ph].
[76] K. Kannike, Eur. Phys. J. C 72 (2012) 2093, arXiv:1205.3781 [hep-ph].
[77] S. Mandal, O. Miranda, G.S. Garcia, J. Valle, X.-J. Xu, Phys. Rev. D 105 (2022), https://doi.org/10.1103/physrevd.105.095020.
[78] C. Bonilla, R.M. Fonseca, J. Valle, Phys. Rev. D 92 (2015), https://doi.org/10.1103/physrevd.92.075028.
[79] A. Arhrib, R. Benbrik, M. Chabab, G. Moultaka, M.C. Peyranère, L. Rahili, J. Ramadan, Phys. Rev. D 84 (2011), https://doi.org/10.1103/physrevd.84.095005.
[80] S. Centelles Chuliá, R. Srivastava, A. Vicente, J. High Energy Phys. 03 (2021) 248, arXiv:2011.06609 [hep-ph].
[81] P. Zyla, et al., Particle Data Group, PTEP 2020 (2020) 083C01, and 2021 update.
[82] A.M. Baldini, et al., MEG, Eur. Phys. J. C 76 (2016) 434, arXiv:1605.05081 [hep-ex].
[83] M.E. Peskin, T. Takeuchi, Phys. Rev. D 46 (1992) 381.
[84] G. Funk, D. O'Neil, R.M. Winters, Int. J. Mod. Phys. A 27 (2012) 1250021, arXiv:1110.3812 [hep-ph].
[85] N. Khan, Eur. Phys. J. C 78 (2018) 341, arXiv:1610.03178 [hep-ph].
[86] S. Mandal, O.G. Miranda, G.S. Garcia, J.W.F. Valle, X.-J. Xu, arXiv:2203.06362 [hep-ph], 2022.
[87] J.R. Forshaw, A. Sabio Vera, B.E. White, J. High Energy Phys. 06 (2003) 059, arXiv:hep-ph/0302256.
[88] J.R. Forshaw, D.A. Ross, B.E. White, J. High Energy Phys. 10 (2001) 007, arXiv:hep-ph/0107232.
[89] S. Chatrchyan, et al., CMS, J. High Energy Phys. 07 (2013) 122, arXiv:1305.0491 [hep-ex].
[90] M. Aaboud, et al., ATLAS, Phys. Rev. D 98 (2018) 032009, arXiv:1804.03602 [hep-ex].
[91] B. Abi, et al., Muon g-2, Phys. Rev. Lett. 126 (2021) 141801, arXiv:2104.03281 [hep-ex].
[92] F. Jegerlehner, A. Nyffeler, Phys. Rep. 477 (2009) 1, arXiv:0902.3360 [hep-ph].
[93] J. Ellis, Comput. Phys. Commun. 210 (2017) 103, arXiv:1601.05437 [hep-ph].